

Etching of MgO crystals in acids: surface micromorphology

K. SANGWAL*, J. N. SUTARIA

Department of Physics, Sardar Patel University, Vallabh Vidyanagar 388120, Gujarat, India

Several etchants based on simple acids are proposed for revealing dislocations on $\{100\}$, $\{110\}$ and $\{111\}$ faces of MgO single crystals. Some acids under different etching conditions are shown to produce etch pyramids at decorated dislocations, while etch hillocks, spherulites and dendrites are formed under different conditions. With increasing concentration of H_2SO_4 , $\langle 110 \rangle$ pits, circular pits, $\langle 100 \rangle$ pits, $\langle 110 \rangle$ pyramids as well as $\langle 100 \rangle$ pits, dendrites and spherulites, and hillocks are formed in that order. Etching characteristics of other acids also showed a more or less identical trend. The observations are interpreted with the assumption that with increasing concentration of acid, an effective undersaturation and later supersaturation is developed very close to the dissolving crystal face. The chemistry of the dissolution process is also discussed.

1. Introduction

The applications of selective etching as a tool in the study of dislocation behaviour are well demonstrated [1, 2], but the basic mechanism of the process is still to be understood. Since the classical work of Gilman *et al.* [3], much work in this direction has appeared in the literature on alkali halides [4-13] as well as on metals [14-17], in which attempts have been made to understand it.

Etching solutions of alkali halides consist of a solvent (usually some alcohol or organic acid) to which an inhibitor is added. The etchants of metals and semiconductors are relatively complicated and consist of at least two solutions. One of these solutions forms a compound with the crystals, while the other desorbs it by forming certain complexes. There is another class of etchants which consists of some pure solutions, e.g. mineral acids for the etching of calcite, fluorite, barite, etc. This class of etchants is not only suitable but also interesting for the study of the etching process because of its simplicity of composition.

By etching, a change in the orientation of the etch pits [3, 4, 6-11, 18, 19] and the formation of elevations have been reported [20-24]. The

change in the morphology of etch pits has generally been interpreted by considering the difference in the rate of removal of atoms along different directions. In some cases the emphasis was mainly on the nucleation and motion of kinks over the surface, whereas in others it was on the arrangement of ions or atoms on the surface. The formation of elevations has also been considered in several works. Honess [25] considers that elevations result due to the interaction of neighbouring etch pits. Buckley [26] agrees with Honess and further states that elevations cannot possess a symmetry related to the crystal face and that the majority of the elevations reported in the literature are, in fact, due to growth. Patel and Goswami [22] reported nearly circular elevations resulting from the protection of the surface from the etchant by gas bubbles. The formation of crystallographic elevations due to interaction of neighbouring pits has also been reported [23]. In cases where there is no evidence of pit interactions, the elevations are believed to occur when the rate of general surface dissolution is more than the rate of dissolution at certain protected spots [27].

* Present address: Institute of Crystallography, Academy of Sciences of the USSR, Leninskii Pros. 59, Moscow V-333, USSR.

Stokes *et al.* [28] employed two solutions based on (1) NH_4Cl and H_2SO_4 and (2) H_2SO_4 to reveal dislocations and polish $\{100\}$ faces of MgO crystals. It was reported [21] that the first etchant at different temperatures developed selective etch pits and asymmetric, non-crystallographic hillocks, whereas the second etchant produced pyramids at impurity segregated dislocations. In our experiments, it was found that addition of NH_4Cl to H_2SO_4 is superfluous: H_2SO_4 alone can form dislocation etch pits on $\{100\}$ faces of MgO and in this respect it is not unique, but several other acids can produce equally good selective etch pits. Invariably the morphology of etch pits was found to change with acid concentration. Many solutions prepared from different acids were observed to form etch pyramids at old dislocations. Some solutions produced hillocks and pyramids. A brief study on the etching of $\{110\}$ and $\{111\}$ faces showed that dislocations emerging on these faces can also be revealed by the etchants of $\{100\}$ faces. The present article systematically deals with these features on MgO crystals and offers a possible mechanism for their formation from the standpoint of chemical reactions.

During the investigations, undoped as well as doped MgO crystals from a number of sources (Norton Research Corporation, Canada; Norton Research Corporation, USA; and AERE, Harwell, UK) were employed. The etching behaviour of $\{100\}$ cleavage face of the crystals was found to be almost alike so far as the development of pits, pyramids, spherulites and hillocks was concerned,

but the general surface dissolution was different for different crystals.

For the studies, $\{100\}$ and $\{110\}$ faces were obtained by cleavage, whereas $\{111\}$ faces were sawn. While cleaving MgO crystals along the $\{100\}$ plane, it was found that the cleavages could easily be obtained by giving a light stroke with a sharp knife positioned along a $\{100\}$ plane. Obtaining $\{110\}$ cleavages by a similar procedure required several trails, somewhat heavier strokes and thinner (0.5 to 1 mm thick) crystal plates. The thermal shock method, in which a corner of a crystal plate heated to 800 to 900° C is slightly immersed in a cold water bath, which is less laborious, was seldom used in view of the introduction of numerous slip bands during the act.

2. Etching of $\{100\}$ cleavages

2.1. Dislocation etch pits

Several solutions of different concentrations of various acids at different temperatures are found to reveal dislocations. The size and shape of etch pits are concentration as well as temperature dependent, the latter dependence being not as marked as that with acid concentration. The distribution of etch pits produced by 0.03 N and 6.35 N H_2SO_4 solutions at 30° C on congruent faces is shown in Fig. 1a and b respectively. The pits have changed over their orientation from $\langle 110 \rangle$ to $\langle 100 \rangle$ directions with an increase in H_2SO_4 concentration. Besides the revelation of sub-boundaries and glide bands by the two solutions, a one-to-one correspondence of etch pits can be

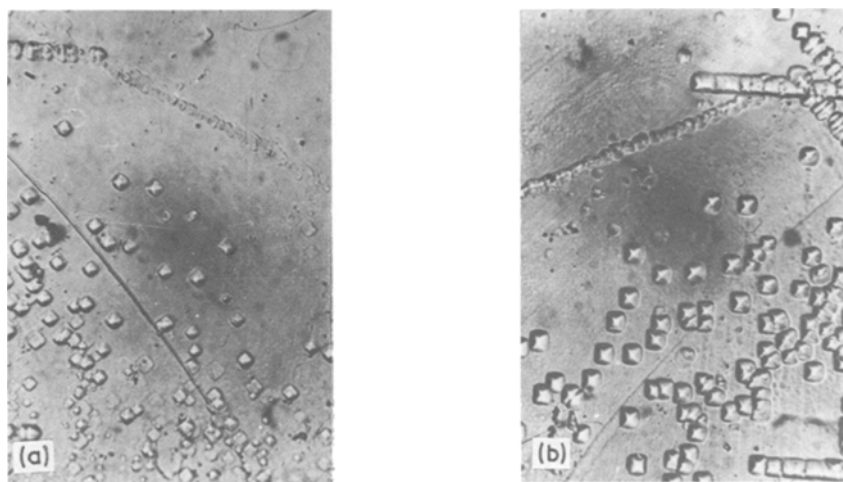


Figure 1 Etch pits produced at 30° C on a matched pair of $\{100\}$ faces (a) 0.03 N H_2SO_4 , (b) 6.35 N H_2SO_4 ; $\times 400$.

TABLE I (a) Etching behaviour of various solutions on $\{100\}$ cleavages

Acid	Normality N	Viscosity η/ρ (cSt)	Etching behaviour
HNO ₃	0.005	1.00	$\langle 110 \rangle$ pits
	0.05	1.0	$\langle 110 \rangle$ pits
	0.5 – 1.0	0.99	circular pits
	3.0	1.01	$\langle 100 \rangle$ pits
	6.2	1.14	$\langle 100 \rangle$ pits
	8.0	1.25	$\langle 100 \rangle$ pits
HCl	0.01	–	$\langle 110 \rangle$ pits
	0.1	1.0	$\langle 110 \rangle$ pits
	1.0 – 2.3	1.04 – 1.09	circular pits
	6.0	1.25	$\langle 100 \rangle$ pits
	12.0	1.77	$\langle 110 \rangle$ pyramids
H ₂ SO ₄	0.01	–	$\langle 110 \rangle$ pits
	0.11	1.01	$\langle 110 \rangle$ pits
	1.13 – 2.60	1.09 – 1.18	circular pits
	6.4	1.52	$\langle 100 \rangle$ pits
	12.7	2.43	$\langle 100 \rangle$ pits
	15.2	2.93	$\langle 100 \rangle$ pits
	18.0	3.90	$\langle 100 \rangle$ pits and $\langle 110 \rangle$ pyramids
	20.25	–	$\langle 110 \rangle$ pyramids
	27	–	dendrites and spherulites
	> 32	–	hillocks
H ₃ PO ₄	1.0	1.08	at room temperature shallow $\langle 100 \rangle$ pits; in boiling solution pits, spherulites and hillocks
	3.7	1.28	shallow $\langle 100 \rangle$ pits at room and boiling temperature
	10.0	2.03	polishes the face
	37.4	–	$\langle 110 \rangle$ pyramids up to 100° C
CH ₃ COOH	1.75	1.20	$\langle 110 \rangle$ pits at room temperature, $\langle 110 \rangle$ pyramids at boiling temperature
	4.0	1.46	$\langle 110 \rangle$ pits
	7 – 10	1.8 – 2.2	circular pits
	14.0	2.55	$\langle 100 \rangle$ pits
	17.5	1.17	$\langle 100 \rangle$ pits
HCOOH	1.76	1.03	$\langle 110 \rangle$ pits up to 100° C
	17.6	1.31	at room temperature $\langle 110 \rangle$ pyramids; in boiling solution both spherulites, pyramids
HCl + CH ₃ COOH; HNO ₃ + CH ₃ COOH (in 1:1 vol. ratio) –		–	$\langle 110 \rangle$ pyramids up to boiling temperature

established on the two faces. This shows that the etch pits mark the emergence points of dislocations.

It should be pointed out that etch pits at new dislocations are larger and deeper than those at old ones. This behaviour was noted for almost all the etchants (except dilute H₃PO₄) and at all the temperatures. The etching behaviour of different acids of various concentrations is illustrated in Table Ia.

2.2. Etch pyramids

Ghosh and Clarke [21] and Bowen [29] reported pyramid-shaped etch hillocks produced by H₃PO₄

acid on $\{100\}$ cleavages formed at elevated temperatures at the sites of impurity precipitation. The pyramids were shown to have their sides parallel to $\langle 110 \rangle$ directions and were randomly distributed on the face.

We conducted experiments using H₃PO₄. It was found that at room temperature, only concentrated H₃PO₄ produced these pyramids. At lower concentrations, very shallow etch pits of $\langle 100 \rangle$ orientations, presumably at old dislocations, were formed. Temperature was not a great factor in their formation. Besides H₃PO₄, several other acid solutions developed the pyramids (see Table Ia). An

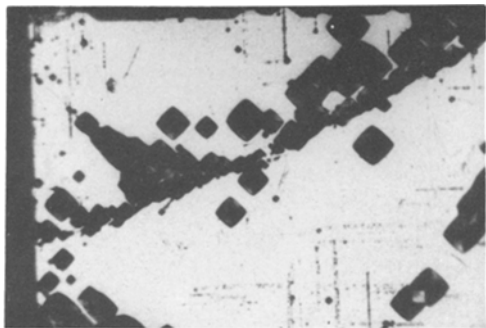


Figure 2 Pyramid formation of 40° C by 37.4 N H₃PO₄; × 350.

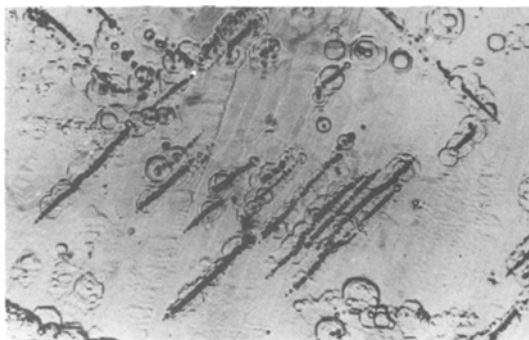


Figure 3 Photograph showing the development of pyramids at dislocations. Etching: 0.5 N H₂SO₄ and 37.4 N H₃PO₄; × 200.

example of pyramid formation at 40° C by 37.4 N H₃PO₄ is shown in Fig. 2. From their appearance at sub-boundaries and slip bands and growth in width and height on prolonged etching (photograph not shown here), it is believed that, in fact, the pyramids reveal dislocations and that their size probably depends on the amount of segregated impurities. To ascertain that the pyramids are at the sites of dislocations, a fresh cleavage was first

etched in a dislocation etchant (0.5 N H₂SO₄) and subsequently in 37.4 N H₃PO₄ to produce pyramids and it was then photographed. Fig. 3 show this. Obviously, the pyramids are located at the emergence points of dislocations, but not all dislocations give rise to pyramids.

The pyramids often exhibited interesting patterns, hitherto never reported, after chemical etching of MgO. They include helicoids, open and closed loops, regular and irregular nets of dislocations and sub-boundaries formed by parallel rows of dislocations. These observations will be reported later.

2.3. Etch hillocks, dendrites and spherulites

Ghosh *et al.* [21] reported hillocks produced by etching MgO cleavages in an etchant composed of a saturated solution of NH₄Cl and conc. H₂SO₄ in a 5:1 ratio by volume at 110° C. At room temperature, we observed similar hillocks at high concentrations (> 32 N) of H₂SO₄. Two examples are shown in Fig. 4. It was invariably noted that the hillocks preferred to develop at cleavage steps. The concentration of these hillocks was also observed to be quite high in doped and surface-damaged crystals.

In the range 25 to 29 N H₂SO₄, spherulites and dendrites were observed to develop, as shown in Fig. 5a. The electron micrograph of one of the spherulites (Fig. 5b), shows that the spherulite-like features are made up of plane sheets, which appear to be deposited on the face. As the acid concentration was increased, the spherulite-like features were reduced in size and became filled-in to yield hillocks. At boiling temperatures, 17.6 N HCOOH and 1 N H₃PO₄ were also observed to produce spherulites. With the former they were accompanied by pyramids, while with the latter by

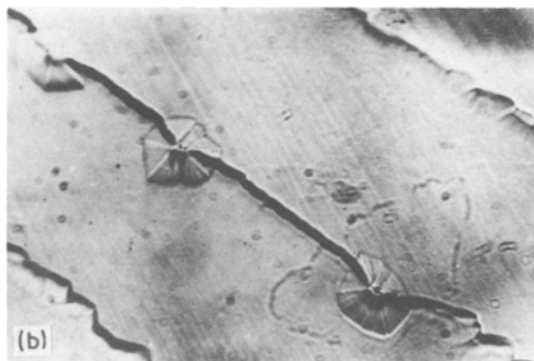


Figure 4 Production of hillocks by conc. H₂SO₄. Temperature of etching 30° C; × 175.

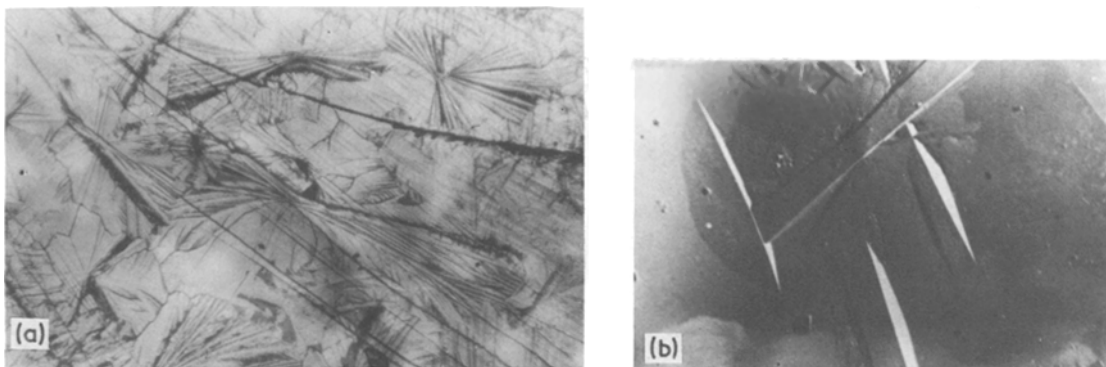


Figure 5 Spherulites and dendrites produced by H_2SO_4 ($N = 25$ to 29). Room temperature $30^\circ C$. (a) Optical photograph, $\times 80$, (b) electron micrograph, $\times 1000$.

hillocks. Fig. 6 shows the examples of the formation of spherulites and pyramids by boiling $17.6 N HCOOH$ and $1.0 N H_3PO_4$ solutions. It should be noted from these figures that the pre-existing cleavage lines lie below the features. This indicates that the features are due to the deposition of some material on the crystal cleavage.

2.4. Material and mode of deposition

To elucidate the nature of the material deposited to form spherulites and hillocks, etching and indentation experiments were carried out on the hillocks. Figs. 7 and 8 show the development of selective etch pyramids by $37.4 N H_3PO_4$ on a hillock and on a spherulite (strictly speaking it is something like a sheaf) formed by H_2SO_4 and $HCOOH$ respectively. Fig. 9 illustrates an indentation rosette pattern generated by indenting the top of a hillock formed by $32 N H_2SO_4$ and subsequent etching in a dislocation etchant. These observations strongly suggest that the hillocks are made up of MgO material itself.

Further experiments in connection with the material and mode of deposition, are reported in Section 5.

3. Etching of $\{110\}$ cleavages

Some of the etching solutions devised for $\{100\}$ cleavages were tried on $\{110\}$ faces. It was observed that at very low concentrations of H_2SO_4 , HNO_3 and HCl , shallow, boat-shaped pits with their axes parallel to $\langle 110 \rangle$ directions were observed. Grain boundaries, slip bands and one-to-one pit correspondence on matched faces were not observed. At slightly higher concentrations, the above characteristics were exhibited by the etch pits, indicating that they had nucleated at dislocations. They were also more or less elliptical in morphology. With further increase in concentration, the etch pits became first somewhat rectangular in outline with their longer sides parallel to $\langle 110 \rangle$ directions, then square, and finally, rectangular and elliptical again but with their longer sides parallel to $\langle 100 \rangle$ directions. Fig. 10a

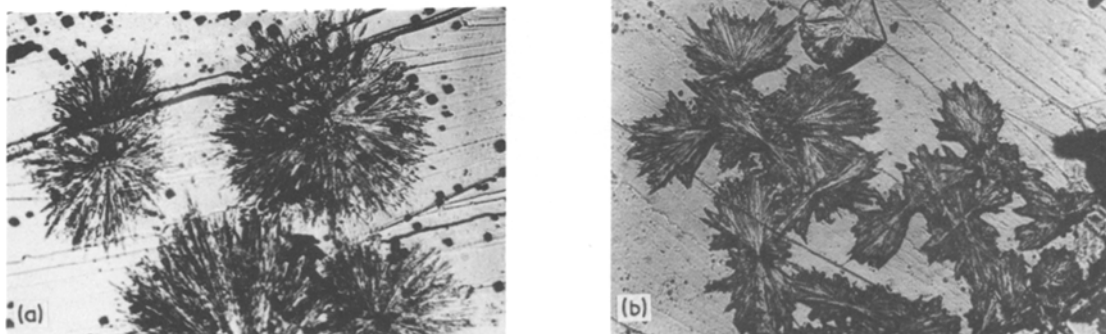


Figure 6 Spherulites and hillocks formed by (a) $17.6 N HCOOH$, (b) $1 N H_3PO_4$. Boiling solutions; $\times 100$.

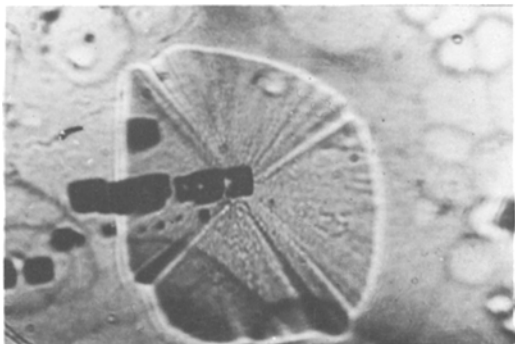


Figure 7 Selective etch pyramids formed by 37.4 N H_3PO_4 on a hillock developed by conc. H_2SO_4 , $\times 800$.

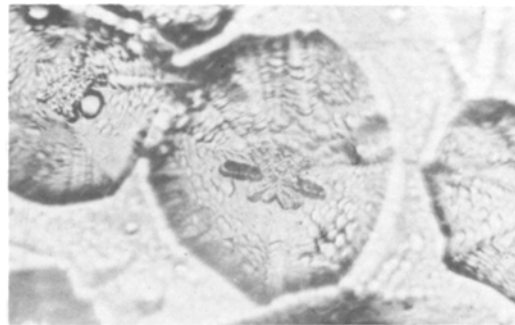


Figure 9 Indentation rosette pattern on a hillock formed by 32 N H_2SO_4 , $\times 800$.

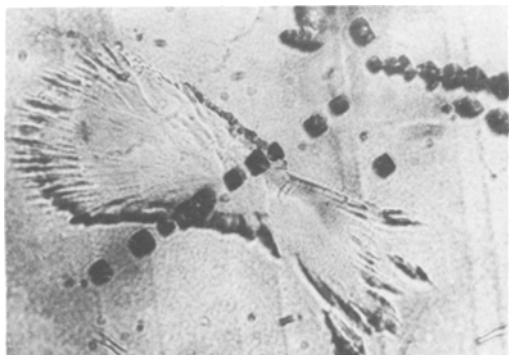


Figure 8 Selective etch pyramids formed by 37.4 N H_3PO_4 on a spherulite resulting due to $HCOOH$, $\times 350$.

and b illustrate the morphology of etch pits on a $\{110\}$ cleavage face etched in 6.35 N H_2SO_4 and 1.13 N H_2SO_4 in succession. That the distribution of etch pits is practically the same indicates that the pits are indeed dislocation etch pits. The

change in the morphology of etch pits caused by H_2SO_4 is shown schematically in Table II.

It should be mentioned that H_3PO_4 also shows the above behaviour upon dilution. At higher temperatures, concentrated H_3PO_4 polishes the face.

4. Etching of $\{111\}$ faces

No significant difference in the etch patterns on $\{111\}$ faces by HNO_3 , HCl and H_2SO_4 was observed. Fig. 11a illustrates an etch pattern produced by 0.34 N H_2SO_4 after 1 h. The morphology of etch pits is more or less triangular. Since the larger pits can be followed on prolonged etching and the arrangement of etch pits along the diagonal of the figure is similar to that of a subboundary, it can be assumed that the etch pits reveal the emergence points of dislocations. Another pattern of etch pits produced by 5.65 N H_2SO_4 is shown in Fig. 11b. The pits in this photograph appear trapezium-shaped, but in fact they are elongated hexagonals.

TABLE II Morphology of etch pits on $\{100\}$ and $\{110\}$ faces in H_2SO_4 solutions: dep = dislocation etch pits

Face	H_2SO_4	0.34N	1.13N	2.6N	4.0N	6.4N	12.7N	21.4N
(100)								
	Results	dep	dep	dep	dep	dep	dep	dep and pyramids
(110)								
	Results	shallow non-dep	dep	dep	dep	dep	dep	dep

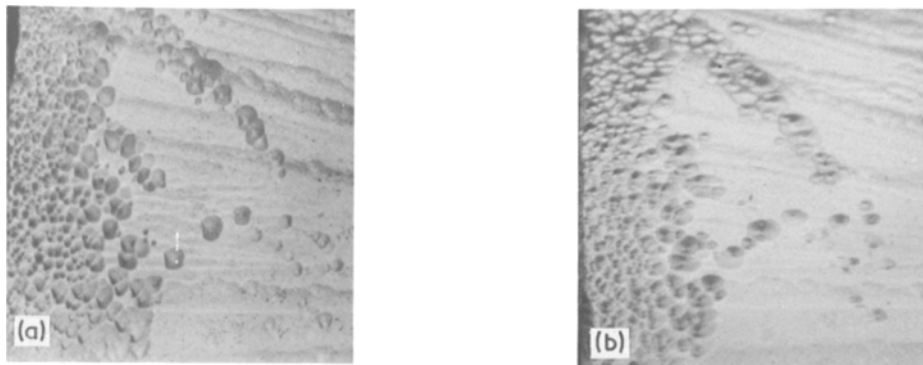


Figure 10 Dislocation etch pits formed on a $\{1\ 1\ 0\}$ cleavage face: (a) 6.35 N H_2SO_4 , (b) 1.13 N H_2SO_4 . Etching temperature 30°C , $\times 250$.

5. Discussion

Crystal dissolution has, in many cases, reverse characteristics in relation to those of growth. Dissolution proceeds under undersaturated conditions whereas growth results under supersaturated conditions. At dislocation sites the local change in the chemical activity leads to the formation of etch pits. As the conditions become more undersaturated the rate of kink nucleation becomes maximal, whereas under less undersaturated conditions it becomes minimal [30]. Consequently, with increasing undersaturation, the morphology of etch pits on $\{1\ 0\ 0\}$ faces is expected to change from $\langle 1\ 0\ 0 \rangle$ orientations to $\langle 1\ 1\ 0 \rangle$ orientations [4]. Increase in the concentration of acid leads to an increase in undersaturation.

Spherulites grow as a result of a rapid increase in supersaturation, but addition of impurities leads to the formation of sheaves [31].

A rearrangement of the observations presented in Table 1a in order of increasing normality (Table 1b) shows that etching behaviour of the acids investigated follows the same pattern. $\langle 1\ 1\ 0 \rangle$ pits are first formed, then circular pits, $\langle 1\ 0\ 0 \rangle$ pits and finally pyramids, dendrites, spherulites and hillocks. To understand the observations, in the above sequence, on the basis of undersaturation and supersaturation, we have to assume that with increasing concentrations of acids, a transition takes place from undersaturation to supersaturation at the crystal-liquid interface. It is indeed very difficult to conceive that increasing concen-

TABLE I (b) Sequence of formation of different etch figures on $\{1\ 0\ 0\}$ face*

Acid	Normality					
	Very low	Low	Moderate	High	Higher	Highest
HNO_3	$\langle 1\ 1\ 0 \rangle$ pits	circular pits	$\langle 1\ 0\ 0 \rangle$ pits	—	—	—
HCl	$\langle 1\ 1\ 0 \rangle$ pits	circular pits	$\langle 1\ 0\ 0 \rangle$ pits	$\langle 1\ 1\ 0 \rangle$ pyramids	—	—
HCOOH	$\langle 1\ 1\ 0 \rangle$ pits	N.I.†	N.I.	$\langle 1\ 1\ 0 \rangle$ pyramids at room temperature, spherulites and $\langle 1\ 1\ 0 \rangle$ pyramids at boiling temperature	—	—
CH_3COOH	$\langle 1\ 1\ 0 \rangle$ pits	circular pits	$\langle 1\ 0\ 0 \rangle$ pits	—	—	—
H_3PO_4	N.I.	N.I.	$\langle 1\ 0\ 0 \rangle$ pits at room temperature, $\langle 1\ 0\ 0 \rangle$ pits and spherulites at boiling point	polishes	polishes	$\langle 1\ 1\ 0 \rangle$ pyramids
H_2SO_4	$\langle 1\ 1\ 0 \rangle$ pits	circular pits	$\langle 1\ 0\ 0 \rangle$ pits	$\langle 1\ 0\ 0 \rangle$ pits and $\langle 1\ 1\ 0 \rangle$ pyramids	dendrites and spherulites	noncrystallographic hillocks

* Unless otherwise stated the observations are for room temperature.

† N.I. = not investigated.

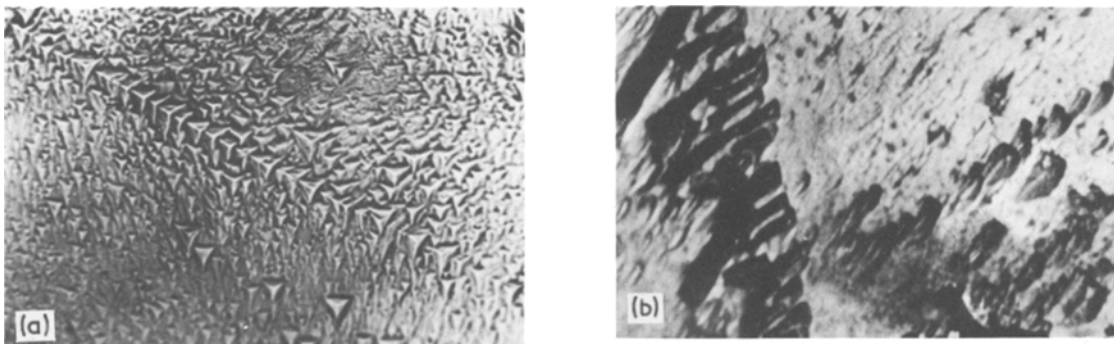


Figure 11 Etch pits on $\{111\}$ face caused by (a) $0.34 \text{ NH}_4\text{SO}_4$ at 33°C , $\times 350$; (b) $5.65 \text{ NH}_4\text{SO}_4$ at 30°C , $\times 420$.

tration should result in increasing undersaturation. To explain the results, we must consider the chemistry of the process taking place at the surface, and the structure of the surface.

The real surfaces may be realized as deformed ones because of the rearrangement of the charge and size of the ions that compose an MgO crystal. The deformed $\{100\}$ surfaces of halite-type crystals consist of oriented dipoles, whose negative ions are directed towards space [32]. The net effect of this rearrangement is to lower the surface free energy. In our case, we are not concerned with this type of lowering because the same type of surface is used in every case. Another factor that may reduce the surface energy is the adsorption of water molecules and reaction products. Adsorption of water is presumably very weak in

halite-type crystals and more so in crystals having ions of low polarizability [32]. The reactivity of O^{2-} ions in initiating the reactions should not be underrated. It is perhaps this reactivity that is responsible for the nucleation of pits, as evidenced by the observation that only solutions having H^+ ions form pits.

Let us consider the arrangement of ions on $\{100\}$ and $\{110\}$ faces of MgO. Fig. 12a and b show the stacking of Mg^{2+} and O^{2-} ions on $\{100\}$ and $\{110\}$ faces respectively. The dark circles show Mg^{2+} and open circles O^{2-} ions. In an ideal case, H^+ combines with an anion* say at O, to form OH^- . This OH^- will combine with another H^+ ion and be desorbed from the site O. The nearest ions around O are Mg^{2+} . These ions are comparatively less strongly bonded to the lattice than the O^{2-} ions and hence will be dissolved away. Then the ions marked 3, 3' and 4 will be dissolved to produce pit A1. The formation of $\langle 100 \rangle$ pits is thus expected to be a normal mode in view of the high activity of $\langle 110 \rangle$ ions in comparison with $\langle 100 \rangle$ ions. High activity is due to the stacking of similarly charged ions and the easy detachment of anions along $\langle 110 \rangle$ directions. This means that the rate of removal of steps formed by $\langle 110 \rangle$ ions (V_{110}) is greater than that formed by $\langle 100 \rangle$ ions (V_{100}).

An interpretation of $\langle 110 \rangle$ pit orientation at high acid dilution may be deduced from the structure of ledges being dissolved away. Reference to Fig. 12a shows that in the octagonal pit outline, the ions stacking along $\langle 110 \rangle$ directions are chemically more active than the ions along $\langle 100 \rangle$ directions, because they have a higher

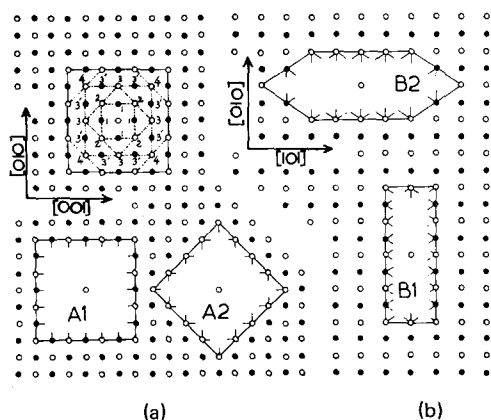


Figure 12 Schematic representation of the removal of atoms on (a) $\{100\}$ and (b) $\{110\}$ face, Open circles, O^{2-} ions; closed circles, Mg^{2+} ions.

* This is a simplified approach. Initially a molecule of MgO should be detached from the dislocation site. However, as the outline of the observable pits lies in the perfect lattice, the simplification is correct.

TABLE III Solubility and heat of formation of some magnesium salts

Salt	Solubility	Heat of formation (kcal mol ⁻¹)	Salt	Solubility	Heat of formation (kcal mol ⁻¹)
MgO	ins*	-143.8	Mg(C ₂ H ₃ O ₂) ₂	hs	-
MgCl ₂ aq.	s†	-190.46	Mg(NO ₃) ₂ aq.	hs	-209.2
MgCl ₂ · H ₂ O	s	-231.2	Mg(NO ₃) ₂ · 6H ₂ O	hs	-624.3
MgCl ₂ · 2H ₂ O	s	-306.0	MgSO ₄ aq.	s	-327.3
MgCl ₂ · 4H ₂ O	s	-390.5	MgSO ₄ · 2H ₂ O	s	-381.9
MgCl ₂ · 6H ₂ O	s	-597.5	MgSO ₄ · 7H ₂ O	s	-808.7
Mg(OH)Cl	-	-191.3	Mg ₃ (PO ₄) ₂	ins	-915.2
Mg(OH) ₂	ins.	-221.0	Mg ₃ (PO ₄) ₂ · 4H ₂ O	vss	-
Mg(CO ₂ H) ₂	s	-	Mg ₃ (PO ₄) ₂ · 8H ₂ O	ss	-

* ins, s, hs, ss and vss mean insoluble, soluble, highly soluble, slightly soluble and very slightly soluble, respectively.

† Solubility of chlorides, nitrates, sulphates and phosphates increases with increasing water of hydration.

number of unsatisfied bonds. The reaction product, say MgCl₂, is expected to have a greater tendency for adsorption (i.e. stay) at such active sites than at the relatively inactive sites, thus reducing V_{110} . Also at low acid concentrations, more water molecules will try to unite with the reaction product, therefore its capability to adsorb at relatively inactive sites will be less. The effect of adsorption of MgCl₂ at inactive sites is to decrease V_{110} while that of the union of water molecules with MgCl₂ is to increase its solubility (Table III). The net effect of these two factors, therefore, is that V_{100} is greater than V_{110} . Successive dissolution and adsorption will result in $\langle 110 \rangle$ pits. At higher acid concentrations, V_{100} will not show an increase because of the sparsity of water molecules and therefore relatively poor adsorption. This mechanism is similar to that described [17, 19, 33].

A number of factors may contribute to the formation of circular or octagonal pits at intermediate concentrations. If the primary product forms a series of higher compounds, as for example PbCl₂, PbCl₄²⁻, PbCl₆⁴⁻, etc, in the case of the etching of PbS [33] or it forms a series of hydrated compounds as in the present case, the pits are expected to be circular. When the product of the reaction does not behave as stated above by virtue of either its chemical properties, or by its modifications by some foreign material added deliberately or segregated to dislocations, octagonal pits develop.

The change in the morphology of etch pits on $\{110\}$ faces can be understood by the above mechanism. The concentration of the etchant at which a transition takes place in the orientation of etch pits is, however, higher for $\{110\}$ faces. To

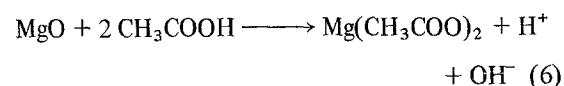
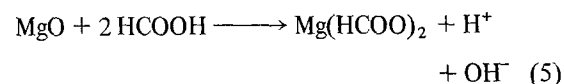
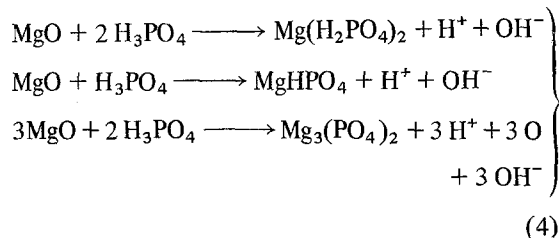
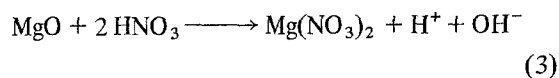
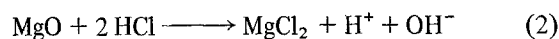
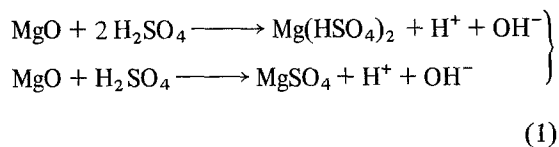
explain this, we should consider the physical state of the two surfaces. The surface energy of $\{110\}$ faces is higher than that of $\{100\}$ face [34]. The trend with which the energies of the two surfaces in contact with the solution falls may be considered similar, because the concentration of the adsorbent and of the solution is the same on both. Consequently, in solution the surface energy of $\{110\}$ faces is always greater than that of $\{100\}$ faces. Since surface energy governs undersaturation [26], this statement means that on a particular face a transition stage is obtained only if the concentration of the solution produces some values of undersaturation.

Examination of Table I shows that in H₂SO₄ spherulites and dendrites form at concentrations of about 27N whereas at above 32N hillocks form. Although the spherulites produced by HCOOH are formed by thin needles whereas those produced by H₂SO₄ are formed by thick plates, the mode of their development appears identical. The spherulites and hillocks develop on the pre-existing surface, and tend to fill the cleavage steps. Features with these characteristics should be considered due to growth and certainly not due to etching, in spite of the fact that etching leads to their formation. Their growth is preferred at cleavage lines (Fig. 4b), although they also grow on relatively flat surfaces (Fig. 4a). To decide the origin and mode of their growth, the following experiments were performed.

A cleavage of MgO was etched in a continuously, strongly stirred solution of conc.H₂SO₄. Neither hillocks nor spherulites were observed to develop. In another experiment, a cleavage face having hillocks (formed without agitation) was

subjected to dynamic etching. All the hillocks were observed to disappear. From an X-ray powder analysis, the material scraped out from the tops of the hillocks was identified as MgO. Thus it is believed that the features result from overgrowth of MgO on its cleavages. The nucleation centres for the growth of the hillocks are surface irregularities (e.g. cleavage kinks, foreign particles, scratches, etc) and not dislocations.

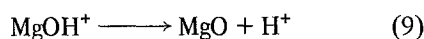
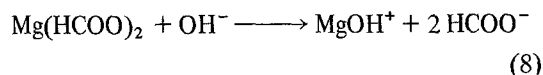
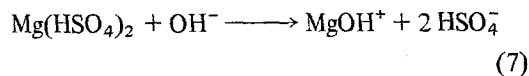
In order to understand the deposition of MgO in acidic solutions, let us write down the chemical reactions between MgO and different acids:



Although hydrosulphate and hydrophosphate are less stable than sulphate and phosphate, they are the more probable reaction products with H_2SO_4 and H_3PO_4 . This is because the first degree dissociation of such acids always gives almost all H^+ ions [35]. Some of the properties of various magnesium salts are given in Table III

[36]. The dissociation constant and dielectric constant of acids are given in Table IV [36].

The generation of MgO from the products of the reactions between acids and MgO itself is not so simple to understand, especially in view of their high solubility. From the products, however, the following reactions can yield MgO:



If the back reactions of the above type are true we should expect similar observations with HNO_3 , HCl and H_3PO_4 . In fact, with a boiling solution of 1 N H_3PO_4 hillocks and spherulites are formed, but not with HNO_3 and HCl .

The degree of dissociation of an acid usually increases with dilution and temperature. This would mean that at high dilutions (or temperatures), the availability of acid ions at the crystal surface is more than at lower dilutions (or temperatures). It follows from this that the higher the dilution is, the higher is the undersaturation. Furthermore, higher solubility of hydrated compounds contributes to a higher undersaturation at higher dilutions. Another factor that is likely to control undersaturation is the diffusion of the reaction products and ions through an interfacial layer, the thickness of which is primarily dependent on the concentration (viscosity) of the solution. Thus, an effective undersaturation is observed which is essentially decided by the relative contribution of these three factors. When the concentration of the acid is increased, the effective undersaturation decreases, and there is a stage when the surface is just polished. Finally, at reasonably high concentrations, supersaturation develops. At low concentrations, the supply of the product of the back reaction to the active sites, e.g. scratches, cleavage

TABLE IV Dissociation and dielectric constants of some solutions

Solution	Degree of dissociation	Dissociation constant	Viscosity η/ρ (cP)	Dielectric constant
HNO_3	0.82 (18° C)	—	1.77 (10° C)	—
HCl	0.784 (18° C)	—	2.00 (30° C)	4.60 (28° C)
H_2SO_4	0.57 (18° C)	1.20×10^{-2} (25° C)	15.70 (30° C)	—
H_3PO_4	0.17 (18° C)	7.52×10^{-3} (25° C)	—	—
HCOOH	—	1.77×10^{-4} (20° C)	1.47 (30° C)	58.5 (16° C)
CH_3COOH	0.004 (18° C)	1.76×10^{-5} (25° C)	1.04 (30° C)	6.15 (20° C)

steps, impurity clusters etc, is absent because of strong diffusion and weak concentration conditions. Under these conditions a local supersaturation is not developed. At higher concentrations, the back reaction product is unable to overcome the viscosity of the solution and hence starts depositing on the face. In essence, spherulites and pyramids form only under conditions when the rate of the product formation is more than that with which the product goes to the main body of the etchant. At higher temperatures in boiling 17.6 N HCOOH and 1.0 N H₃PO₄ acids, such a situation also probably arises, although in principle, undersaturation should develop here.

Pyramids were always found to develop at decorated dislocations, irrespective of their type. Decorated dislocations also always gave shallow pits. It is logical to assume, therefore, that impurities hinder dissolution at dislocations. Etch pyramids are, therefore, believed to form as a consequence of the greater rate of surface dissolution than that at the dislocations.

6. Conclusions

Apart from the report of several solutions which produce dislocation etch pits, the following conclusions can be drawn from this study:

(1) The formation of pits of different morphologies is associated with different effective undersaturation developed very close to the dislocation sites, whereas spherulites and hillocks result when an effective supersaturation develops at the crystal surface. The formation of spherulites and hillocks is due to a process similar to overgrowth of MgO itself on its cleavages.

The hillocks formed by conc. H₂SO₄ may be treated as filled-in dendrites and spherulites. In the case of etching, the lateral spread of the features is hindered because of the restricted motion of the growing molecules due to the high viscosity of the surrounding liquid. Under dynamic conditions, the velocity of the motion of the solution is increased. This motion increases the dispersal of the reaction products from the crystal face, and therefore, no hillocks are formed under these conditions. Thus spherulites, sheaves and hillocks formed by H₂SO₄, HCOOH and H₃PO₄ are produced by a group of nuclei localized at a point or from a platy crystal.

(2) In acidic solutions, etch pits are produced under conditions when the solutions have a low

viscosity and the reaction products are moderately soluble. High viscosity of the solutions usually leads to the formation of spherulites and hillocks.

(3) By an increase in the concentration or temperature of the solution, a change over from etching to growth takes place. Although an attempt has been made to interpret the obtained results, a confirmation of the reaction products proposed here is desirable by their direct observation at the crystal-solution interface.

Acknowledgements

We wish to thank Professor A. R. Patel for his guidance and interest in the work, and Professor K. G. Bangsiger, Dr A. A. Urusovskaya and Dr S. K. Arora for useful discussions with K. S. We also thank Drs S. M. Patel and T. C. Patel who not only encouraged us but took a number of the photographs illustrated here.

References

1. W. G. JOHNSTON, "Progress in Ceramic Science", Vol. 2 (pergamon Press, 1962).
2. YU. I. PSHENICHNOV, "Revelation of the Fine Structure of Crystals" ("Metallurgia" Press, Moscow, 1974) in Russian.
3. J. J. GILMAN, W. G. JOHNSTON and G. W. SEARS, *J. Appl. Phys.* **29** (1958) 747.
4. M. B. IVES, *J. Phys. Chem. Solids* **24** (1963) 275.
5. M. B. IVES and J. P. HIRTH, *J. Chem. Phys.* **33** (1960) 517.
6. V. N. ROZHANSKII, E. V. PARVOVA, V. M. STEPANOVA and A. A. PREDVODITELEV, *Kristallogr.* **6** (1962) 704.
7. A. A. URUSOVSKAYA, *ibid* **8** (1963) 75.
8. R. THYAGARAJAN and A. A. URUSOVSKAYA, *J. Phys. Chem. Solids* **28** (1967) 1257.
9. E. YU. GUTMANAS and E. M. NADGORNYYI, *Kristallogr.* **13** (1968) 114.
10. V. HARI BABU and K. G. BANSIGIR, *J. Phys. Chem. Solids* **30** (1968) 1015.
11. V. HARI BABU and K. G. BANSIGIR, *J. Crystal Growth* **2** (1968) 8.
12. I. V. K. BHAGAWAN RAJU and K. G. BANSIGIR, *ibid* **11** (1971) 171.
13. I. V. K. BHAGAWAN RAJU and K. G. BANSIGIR, *ibid* **15** (1972) 288.
14. A. A. PREDVODITELEV and E. G. POPKOVA, Collected works in the series "Crystal Growth", Vol. 5, edited by N. N. SHEFTAL ("Nauka" press, Moscow 1965) p. 259, in Russian.
15. E. G. POPKOVA, G. S. MATVEEVA and A. A. PREDVODITELEV, *Kristallogr.* **14** (1969) 53.
16. E. G. POPKOVA and A. A. PREDVODITELEV, *ibid* **15** (1970) 91.
17. *Idem*, *ibid* **17** (1972) 612.

18. A. R. PATEL and R. P. SINGH, *J. Crystal Growth* **2** (1968) 373.
19. K. SANGWAL, *Kristallogr.* **20** (1975) 116.
20. B. W. BATTERMAN, *J. Appl. Phys.* **28** (1957) 1236.
21. T. K. GHOSH and F. J. P. CLARK, *Brit. J. Appl. Phys.* **12** (1961) 44.
22. A. R. PATEL and K. N. GOSWAMI, *Proc. Phys. Soc.* **79** (4) (1962) 848.
23. A. R. PATEL and T. C. PATEL, *J. Appl. Crystallogr.* **4** (1971) 207.
24. KOTUHIKO HONDA and TOMO HIROKAWA, *Jap. J. Appl. Phys.* **11** (1972) 1763.
25. A. P. HONESS, "The Nature, Origin and Interpretation of Etch Figures on Crystals" (Wiley, New York, 1927).
26. H. E. BUCKLEY, "Crystal Growth" (Wiley, New York and London, 1958).
27. J. W. FAUST JUN., "The Surface Chemistry of Metals and Semiconductors", edited by H. C. GATOS (Wiley, New York and London, 1960) pp. 151-69.
28. R. J. STOKES, T. L. JOHNSON and C. H. LI, *Phil. Mag.* **3** (1958) 718; **4** (1959) 920.
29. D. H. BOWEN, *Trans. Brit. Ceram. Soc.* **62** (1963) 771.
30. N. CABRERA, "The Surface Chemistry of Metals and Semiconductors", edited by H. C. GATOS (Wiley, New York and London, 1960) pp. 71-81.
31. A. V. SHUBNIKOV and V. F. PARVOV, "The Origin and Growth of Crystals" ("Nauka" press, Moscow, 1969) in Russian.
32. W. A. WEYL, "Structure and Properties of Solid Surfaces", edited by R. GOMER and C. S. SMITH (University of Chicago Press, 1953) pp. 147-84.
33. K. SANGWAL, Ph. D. Thesis, Sardar Patel University (1971).
34. F. SEITZ, "Modern Theory of Solids" (McGraw Hill, New York, 1940) pp. 76-8.
35. YA. I. GERASIMOV, V. P. DREVING, E. N. EREMIN, A. V. KISELEV, V. P. LEBEDEV, G. M. PANCHENKOV and A. I. SHLYGIN, "Course of Physical Chemistry" Vol. 1 ("Khimiya" press, Moscow, 1970), p. 484, in Russian.
36. C. D. HODGMAN, Ed., "Handbook of Chemistry and Physics" (Chemical Rubber Co., Cleveland, Ohio, 1959).

Received 23 January and accepted 3 May 1976.